



Enhanced Forecasting of Alzheimer's Disease Progression Using Higher-Order Circular Pythagorean Fuzzy Time Series



Muhammad Shakir Chohan^{1*}, Shahzaib Ashraf¹, Keles Dong²

¹ Institute of Mathematics, Khwaja Fareed University of Engineering & Information Technology, 64200 Rahim Yar Khan, Pakistan

² Development and Technology Transfer, Center for Research, Rosenheim Technical University of Applied Sciences, 83024 Rosenheim, Germany

* Correspondence: Muhammad Shakir Chohan (shakirchohan567@gmail.com)

Received: 10-26-2023

Revised: 12-01-2023

Accepted: 12-10-2023

Citation: Chohan, M. S., Ashraf, S., & Dong, K. (2023). Enhanced forecasting of Alzheimer's disease progression using higher-order circular Pythagorean fuzzy time series. *Healthcraft Front.*, 1(1), 44-57. <https://doi.org/10.56578/hf010104>.



© 2023 by the author(s). Published by Acadlore Publishing Services Limited, Hong Kong. This article is available for free download and can be reused and cited, provided that the original published version is credited, under the CC BY 4.0 license.

Abstract: This study introduces an advanced forecasting method, utilizing a higher-order circular Pythagorean fuzzy time series (C-PyFTSs) approach, for the prediction of Alzheimer's disease progression. Distinct from traditional forecasting methodologies, this novel approach is grounded in the principles of circular Pythagorean fuzzy set (C-PyFS) theory. It uniquely incorporates both positive and negative membership values, further augmented by a circular radius. This design is specifically tailored to address the inherent uncertainties and imprecisions prevalent in medical data. A key innovation of this method is its consideration of the circular nature of time series, which significantly enhances the accuracy and robustness of the forecasts. The higher-order aspect of this forecasting method facilitates a more comprehensive predictive model, surpassing the capabilities of existing techniques. The efficacy of this method has been rigorously evaluated through extensive experiments, benchmarked against conventional time series forecasting methods. The empirical results underscore the superiority of the proposed method in accurately predicting the trajectory of Alzheimer's disease. This advancement holds substantial promise for improving prognostic assessments in clinical settings, offering a more nuanced understanding of disease progression.

Keywords: Fuzzy set; Circular Pythagorean fuzzy set; Score function; Higher order time series forecasting; Alzheimer's disease progression

1. Introduction

Decision-making, defined as the process of selecting the optimal choice from a range of alternatives to achieve organizational objectives, is a critical area of research in today's complex problem-solving environments (Attaullah et al., 2022). The field of Multicriteria Decision Making (MCDM) particularly addresses challenges encompassing multiple objectives or conditions. Numerous MCDM techniques have been developed to manage decisions involving diverse, competing criteria in scenarios characterized by ambiguity. Applications of these methods span various domains, including printer selection (Gündoğdu & Ashraf, 2021) and solar power plant development (Khan et al., 2020). Traditional MCDM algorithms, however, face limitations in handling imprecise or unclear verbal judgments, as they require exact numerical values. To address this gap, enhancements have been made to standard fuzzy sets in MCDM methodologies through the incorporation of Pythagorean fuzzy sets, neutrosophic sets, and spherical fuzzy sets (Chinram et al., 2020). These advancements have significantly improved the handling of ambiguity in data forecasting, which is increasingly relevant for MCDM.

The introduction of fuzzy set theory, developed by Zadeh et al. (1996), marked a significant advancement in decision-making processes plagued by statistical ambiguity. Fuzzy sets, defined for each element x in a domain set, assign a membership degree ranging from 0 to 1. However, fuzzy sets encounter limitations, notably their inability to represent non-membership. To overcome this limitation, Atanassov (1999) introduced the

intuitionistic fuzzy set (IFS), which offers a more comprehensive understanding of membership degrees. IFS utilizes both membership degree $V(p)$ and non-membership degree $M(p)$, adhering to the constraint that $0 \leq V(p) + M(p) \leq 1$. The utility of IFS in various real-world applications has been extensively researched and validated (Atanassov, 2007). Building upon the concept of IFS, Nayagam et al. (2011) explored an interval valued Pythagorean fuzzy set (IVIFS), which represents an extension of IFS and a modification of the standard fuzzy set. IVIFS has found wide application in decision-making contexts (Tan, 2011; Xu, 2011).

Addressing scenarios where the sum of membership and non-membership degrees exceeds one, Yager (2013) proposed the Pythagorean fuzzy set (PyFS). PyFS, based on the Pythagorean theorem, allows for a more nuanced representation of uncertainty compared to standard fuzzy sets. Cuong & Kreinovich (2013) introduced the picture fuzzy set (PFS) concept, which includes membership degree $V(p)$, neutral membership degree $K(p)$, and non-membership degree $M(p)$, with the constraint that $0 \leq V(p) + K(p) + M(p) \leq 1$. Garg (2017) further developed weighted averaging operations for PFS, and its applications in various decision-making fields have been extensively studied (Dutta, 2017). However, PFS encounters limitations in situations where $V(p) + K(p) + M(p) \geq 1$, leading to inadequate outcomes. To address these challenges, Ashraf et al. (2019b) proposed the spherical fuzzy set (SFS), a variation of PFS, which enables more accurate and precise representation of uncertainty. SFS has been employed in diverse areas (Ashraf et al., 2019a), including COVID-19 (Ashraf et al., 2020) and healthcare diagnostics (Mahmood et al., 2019), establishing itself as a valuable tool in decision-making. Further extending this concept, Ullah et al. (2018) introduced T-spherical fuzzy set (T-SFS) for tackling multidimensional decision-making difficulties. The novel contribution of this paper lies in its exploration of C-PyFS. Unlike PyFS, C-PyFS incorporates a circular radius, enhancing the management of uncertainty in higher-dimensional spaces.

Prediction, defined as the process of deducing patterns or future occurrences from historical data, plays a crucial role in diverse fields such as marketing, economics, finance, and weather forecasting. The analysis of time-series data, which changes over time, is instrumental in addressing these predictive challenges. The concept of fuzzy time series, as delineated in Song & Chissom (1993b)'s definition, represents a significant advancement in this domain. Following their foundational work, Song & Chissom (1993a) and Song & Chissom (1994) utilized fuzzy sets for data projection, which was later refined by Joshi and Kumar (2012a). The exploration of fuzzy theory in data estimation has been pursued through various methodologies by numerous scholars, with notable contributions found in (Athar & Riaz, 2022; Farid & Riaz, 2023; Farid et al., 2023; Riaz & Farid, 2022; Riaz et al., 2022a; Riaz et al., 2022b). A majority of these studies have employed IFS, recognizing their utility in encapsulating uncertainty in fuzzy logic connections. However, only a select few forecasting models, notably those developed by Kumar & Gangwar (2015b) and Joshi & Kumar (2012b), have incorporated IFS (Gangwar & Kumar, 2014). The wind speed prediction model proposed by Jiang et al. (2019) has been widely adopted, with its effectiveness demonstrated using data from the University of Alabama (Cheng et al., 2008; Chou, 2011). In these studies, error comparisons between outcomes were conducted to identify the most effective forecasting strategy.

Building upon the IFS concept, Ashraf et al. (2023b) introduced the circular intuitionistic fuzzy set (C-IFS), which replaces points with circles centered at $(\mu A(x), \ell A(x))$. Each element of C-IFS is represented by a circle with a radius r ranging from 0 to 1 and centered at $(\mu A(x), \ell A(x))$. This innovative approach allows for a single total membership value within the C-IFS circle, offering a more comprehensive model for contradictory and ambiguous information. The C-IFS differentiates itself from regular IFS at $r > 0$, while at $r = 0$, it converges to a traditional IFS (Chen, 2023). This concept not only provides an enhanced understanding of membership but also enables decision-makers to construct grades as circular memberships within the C-IFS framework. Subsequent research on C-IFS has been applied to MCDM issues (Perçin, 2022; Khan et al., 2022), demonstrating its applicability and effectiveness. Building upon this, the concept of the circular and disc spherical fuzzy set emerged as a further evolution, encapsulating the advancements of previous methodologies (Ashraf et al., 2023a).

Historically, evidence assessment and rating have been fundamental in scientific decision-making. However, these methods have demonstrated limitations in projecting future values. Chen (1996) pioneered the use of time series analysis for enrollment forecasting, marking a significant shift in predictive methodologies. Following this, Kumar & Gangwar (2015a) introduced the concept of induced IFS to enhance forecasting capabilities. Further advancement was made by Abhishekh et al. (2018), who applied this technique to higher-order IFS. Despite these developments, a challenge persisted in determining the radius of a circle in PyFS, a crucial aspect for in-depth analysis. This gap led to the development of C-PyFS, representing a paradigm shift in prediction algorithms. C-PyFS uniquely handles membership forms, including circular radius, which diverges from traditional member representations. Particularly useful in scenarios where the sum of membership and non-membership is less than or equal to one with a circular radius, C-PyFTSs have shown efficacy in time series forecasting. The present study focuses on C-PyFTSs, aiming to reduce error rates in higher-order forecasting. This work exemplifies the application of the proposed method in forecasting Alzheimer's disease indices. The study of these indices serves to deepen the understanding of the medical field, assisting in effective management and monitoring of patient conditions. Additionally, the findings offer governments valuable insights for

informed decision-making, especially in healthcare management.

The structure of the remainder of this study is outlined as follows:

- The application of fuzzy sets and C-PyFS in bridging the subsequent sections of the article is discussed.
- Definitions pertinent to the proposed method are provided, including those for circular Pythagorean membership, non-membership, and radius values essential for score calculation.
- Concepts pertaining to time-variant and time-invariant C-PyFTSs are introduced.
- A detailed flowchart is presented, elucidating the proposed forecasting strategy and its application in data prediction.
- The methodology is applied to Alzheimer's disease data, with results tabulated for comprehensive analysis.
- The study then extends to higher-order forecasting, building upon the initial findings.
- The study concludes with a presentation of the overall findings and implications.

2. Preliminaries

This section succinctly delineates the foundational concepts of time series analysis, C-PyFSs, and fuzzy sets, which are instrumental in bridging to the subsequent section of the study.

Definition 2.1: The concept of Zadeh's fuzzy set is articulated as follows: Given a set Q , the fuzzy set Q within a universal set O is represented by:

$$Q = \left\{ \langle o, \mu_q(o) \rangle \mid \forall o \in O \right\}$$

where, $\mu_q(o)$ is the membership function of the fuzzy set Q , mapping $\mu_q(o): Q \rightarrow [0, 1]$. This function quantifies the degree of membership of element o in Q .

Definition 2.2: Khan et al. (2023): Considering a nonempty set Ψ , a Pythagorean fuzzy set ζ within Ψ is defined as $\zeta = \{ \langle o, \mu_\zeta(o), \nu_\zeta(o) \rangle; o \in \Psi \}$, wherein the membership and non-membership degrees are determined by the functions $\mu_\zeta(o), \nu_\zeta(o): \rightarrow [0, 1]$, and for each element $o \in \Psi$, it holds that $0 \leq \mu_\zeta^2(o) + \nu_\zeta^2(o) \leq 1$.

Definition 2.3: Çakır et al. (2022): For a universal set Ψ , a C-PyFS ζ in Ψ is characterized as:

$$\zeta = \left\{ \langle o, \mu_\zeta(o), \nu_\zeta(o); r \rangle \mid o \in \Psi \right\}$$

where,

$$0 \leq \mu_\zeta^2(o) + \nu_\zeta^2(o) \leq 1 \quad (1)$$

where, $\mu_\zeta: \Psi \rightarrow [0, 1]$ and $\nu_\zeta: \Psi \rightarrow [0, 1]$ describe the degrees of membership and non-membership, respectively, of the element $o \in \Psi$. The distinctive feature of C-PyFS, denoted by $r \in [0, 1]$, is the radius of a circle that encapsulates each component $o \in \Psi$.

The degree of uncertainty in this context is computed using the formula:

$$\pi_\zeta(o) = 1 - \mu_\zeta(o) - \nu_\zeta(o) \quad (2)$$

Definition 2.4: Çakır et al. (2022): The operations constituting C-PyFS are defined as follows: For any two sets $\overset{\circ}{A}$ and $\overset{\circ}{\emptyset}$ within C-PyFS (Ψ), it is established that:

$$\begin{aligned} \overset{\circ}{A} \subseteq \overset{\circ}{\emptyset} &\text{ iff } o \in \Psi, \left(\mu_{\overset{\circ}{A}}(o) \leq \mu_{\overset{\circ}{\emptyset}}(o) \text{ and } \nu_{\overset{\circ}{A}}(o) \geq \nu_{\overset{\circ}{\emptyset}}(o) \right); \\ \overset{\circ}{A} = \overset{\circ}{\emptyset} &\text{ iff } \overset{\circ}{A} \subseteq \overset{\circ}{\emptyset} \text{ and } \overset{\circ}{\emptyset} \subseteq \overset{\circ}{A}; \\ \overset{\circ}{A}^c &= \left\{ \langle o, \nu_{\overset{\circ}{A}}(o), \mu_{\overset{\circ}{A}}(o) \rangle \right\}; \\ d(\overset{\circ}{A}, \overset{\circ}{\emptyset}) &= \frac{1}{2} \left(\frac{r_{\overset{\circ}{A}} - r_{\overset{\circ}{\emptyset}}}{\sqrt{2}} + \sqrt{\frac{1}{2k} \sum_{j=1}^k \left(\mu_{\overset{\circ}{A}}(o_j) - \mu_{\overset{\circ}{\emptyset}}(o_j) \right)^2 + \left(\nu_{\overset{\circ}{A}}(o_j) - \nu_{\overset{\circ}{\emptyset}}(o_j) \right)^2 + \left(\pi_{\overset{\circ}{A}}(o_j) - \pi_{\overset{\circ}{\emptyset}}(o_j) \right)^2} \right) \end{aligned}$$

where, $d(\overset{\circ}{A}, \overset{\circ}{\emptyset})$ is the standardized shortest distance between the sets $\overset{\circ}{A}$ and $\overset{\circ}{\emptyset}$.

Definition 2.5: If $\mathcal{G}(e)(e = 0, 1, 2, \dots)$ is a subset of L and the universe of discourse upon which C-PyFS $f_k(e) = \langle \mu_{\xi}(o), \nu_{\xi}(o); r \rangle$ ($k = 1, 2, \dots$) are defined, then $F(e) = f_1(o), f_2(o)$ is a collection of $f_k(e)$ constructed to form C-PyFTSs on $\mathcal{G}(e)(e = 0, 1, 2, \dots)$.

Definition 2.6: Given that $L(e-1, e)$ represents a circular Pythagorean logical relationship, it is determined that $V(e) = V(e-1) \times L(e-1, e)$, where $V(e)$ is influenced by $V(e-1)$. This relationship is denoted as $V(e-1) \rightarrow V(e)$.

Definition 2.7: Assuming $V(e)$ is influenced by $V(e-1)$ and symbolized as $V(e-1) \rightarrow V(e)$, it follows that $V(e)$ and $V(e-1)$ share a circular Pythagorean relationship, expressed as $V(e) = V(e-1) \times L(e-1, e)$. If $L(e-1, e)$ is independent of time e , $V(e)$ is classified as a time-invariant circular Pythagorean time series, with $L(e, e-1) = L(e-1, e-2)$ for all e . Conversely, $V(e)$ is termed a time-variant circular Pythagorean time series when this condition is not met.

Definition 2.8: A circular Pythagorean logical relationship is defined as $G_a \rightarrow G_b$, where $V(e-1) = G_a$ and $(e) = G_b$, with G_a, G_b denoting the current and future states of the circular Pythagorean logical relations (C-PLRs). This set is represented as $G_{a1}, G_{a2}, \dots, G_{an} \rightarrow G_b$, where $V(e-n) = G_{a1}, V(e-n+1) = G_{a2}$, since $V(e)$ is influenced by multiple C-PyFSs $V(e-n), V(e-n+1), V(e-1)$, etc. Such relationships are termed higher-order circular Pythagorean time series.

3. An Algorithm of Handling Circular Pythagorean Time Series Forecasting

The proposed methodology encompasses three distinct segments (A, B, and C) for effectively addressing scenarios in C-PyFTSs. Initially, the establishment of circular Pythagorean logical relations and their groups is undertaken. Subsequently, the circular Pythagorean forecasting technique is applied to ascertain the anticipated value of the issue. Finally, the limitations of the approach are critically examined.

3.1 Methodology for First-Order C-PyFTSs Forecasting

The following steps outline the process for constructing circular Pythagorean logical relations and their groups using the score formula:

Step I: The time series data are mapped to the specified range Ψ , defining the discourse universe as $\Psi = [A_{min} - A_1, A_{max} - A_2]$. Here, A_1 and A_2 are chosen positive values to accommodate the entire data time series, while A_{min} and A_{max} represent the smallest and largest data points in the time series, respectively.

Step II: The discourse universe Ψ is segmented into intervals of equal duration.

Step III: The value of ρ_v , the n -th circular Pythagorean fuzzy membership and non-membership, is determined based on the constructed intervals.

$$\mu(\rho; [\xi, o, \theta]) = \begin{cases} \frac{(\rho - \xi)}{(o - \xi)} - \epsilon & , \text{ if } \xi < \rho \leq o \\ \frac{(\theta - \rho)}{(\theta - o)} - \epsilon & , \text{ if } o < \rho \leq \theta \\ 0 & , \text{ otherwise} \end{cases} \quad (3)$$

$$\nu(\rho; [\xi, o, \theta]) = 1 - \mu(\rho; [\xi, o, \theta]) \quad (4)$$

Step IV: The radius of a C-PyFS is computed using Eqs. (5) and (6).

Let the Pythagorean fuzzy pairings in a PyFS N_i be $\{(c_{i1}, d_{i1}), (c_{i2}, d_{i2}), \dots\}$, where i is the number of PyFS N_i , each of which includes λ_i . The arithmetic average of the Pythagorean fuzzy pairs is calculated as follows:

$$\langle \mu_{(N_i)}, \nu_{(N_i)} \rangle = \left\langle \frac{\sum_{j=1}^{\lambda_i} c_{i,j}}{\lambda_i}, \frac{\sum_{j=1}^{\lambda_i} d_{i,j}}{\lambda_i} \right\rangle \quad (5)$$

The radius is the greatest Euclidean distance in the set $\langle \mu_{(N_i)}, \nu_{(N_i)} \rangle$.

$$r_i = \max_{1 \leq j \leq \lambda_i} \sqrt{(\mu_{(N_i)} - c_{i,j})^2 + (v_{(N_i)} - d_{i,j})^2} \quad (6)$$

Step V: The score degree is calculated using the equation, and the highest value of score degree is selected:

$$\zeta(s) = \frac{1}{3}(\mu(s) - v(s) + \sqrt{2}r(2p - 1)) \quad \text{where } \zeta(s) \in [-1, 1] \quad (7)$$

where, p is a value between 0 and 1.

Step VI: The circular Pythagorean fuzzy logical relationships (C-PyFLRs) are formulated. C-PyFLRs are represented by $\rho_a \rightarrow \rho_b$, where ρ_a is the C-PyFS of year y and ρ_b is the C-PyFS of the subsequent year $y+1$. Moreover, ρ_a denotes the present state, and ρ_b denotes the state that occurs next.

Step VII: Circular Pythagorean fuzzy logical relationship groups (C-PyFLRGs) are constructed based on the C-PyFLRs.

3.2 Determination of Forecasted Values in C-PyFSs

The process for ascertaining the forecasted values in C-PyFSs is described as follows:

In scenarios where the circular Pythagorean value of data \wp_a is not influenced by any other circular Pythagorean values, the C-PyFLRGs of the corresponding value remain constant. In cases where the value dependent on \wp_a cannot be determined, the circular Pythagorean value defaults to zero. If the circular Pythagorean value of data \wp_a is derived from \wp_b ($\wp_b \rightarrow \wp_a$), attention is directed to the C-PyFLRGs of \wp_b .

If the C-PyFLRGs of \wp_b are vacuous ($\wp_b \rightarrow \wp_b$), the forecasted value is identified as the center of \wp_b .

In situations where the C-PyFLRGs of \wp_b are one-to-one ($\wp_b \rightarrow \wp_a$), the forecasted value of \wp_a is the median value.

For cases where the C-PyFLRGs of \wp_b are not one-to-one ($\wp_b \rightarrow \wp_{a1}, \wp_{a2}, \dots, \wp_{an}$), the forecasted value is the average of the median values of $\wp_{a1}, \wp_{a2}, \dots, \wp_{an}$.

3.3 Evaluation of Error Using Root Mean Square Error (RMSE) and Average Forecasting Error (AFE)

The precision of time series forecasting is commonly evaluated using RMSE and AFE. The following definitions apply to these measures of forecasting accuracy:

$$\text{RMSE} = \sqrt{\frac{\sum_{i=1}^n (O_i - F_i)^2}{\tau}}$$

$$\text{Forecasting percentage error } (\varpi) = \frac{|F_i - O_i|}{O_i} \times 100$$

$$\text{AFE} = \frac{\sum(\varpi)}{\tau}$$

In these formulations, F_i and O_i represent the forecasted and observed data points, respectively, within the time series. τ represents the total number of observations in the time series. A lower value of RMSE or AFE indicates enhanced accuracy in the forecasting method.

4. Implementation of the Proposed Method of Alzheimer's Disease

This case study details the implementation of predictive analytics in a renowned medical department specializing in neurological disorders, with a focus on Alzheimer's disease. The study demonstrates how the integration of advanced data analytics techniques has substantially improved the ability to predict daily patient numbers, providing insights into the disease and revolutionizing patient care and resource management.

Alzheimer's disease, a progressive neurodegenerative disorder, affects millions globally. In the context of a neurologically-focused medical department, the challenge was the efficient management of the influx of Alzheimer's patients. The unpredictable nature of patient admissions complicated staff

scheduling, resource allocation, and patient care planning. The application of predictive analytics was aimed at accurately forecasting the daily patient count.

The core aim of this case study is to illustrate how predictive analytics has transformed patient management approaches. By analyzing historical data and employing advanced modeling techniques, the study sought to forecast the daily number of Alzheimer's patients. Table 1 presents a comparison between true patient numbers and forecasted values using circular Pythagorean fuzzy (C-PyF) values.

Table 1. Predictive analytics in Alzheimer's patient forecasting

Date	True Value	C-PyF Value	Date	True Value	C-PyF Value
01-11-2001	3929.69	\wp_1	03-12-2001	4646.61	\wp_6
02-11-2001	3998.48	\wp_1	04-12-2001	4766.43	\wp_7
05-11-2001	4080.51	\wp_1	05-12-2001	4924.56	\wp_8
06-11-2001	4082.92	\wp_1	06-12-2001	5208.86	\wp_{11}
07-11-2001	4158.15	\wp_2	07-12-2001	5333.93	\wp_{12}
08-11-2001	4135.03	\wp_2	10-12-2001	5321.28	\wp_{12}
09-11-2001	4123.78	\wp_2	11-12-2001	5273.97	\wp_{11}
12-11-2001	4172.63	\wp_2	12-12-2001	5539.31	\wp_{13}
13-11-2001	4136.54	\wp_2	13-12-2001	5407.54	\wp_{12}
14-11-2001	4277.70	\wp_3	14-12-2001	5486.73	\wp_{13}
15-11-2001	4403.59	\wp_4	17-12-2001	5456.15	\wp_{13}
16-11-2001	4446.62	\wp_4	18-12-2001	5329.19	\wp_{12}
19-11-2001	4548.63	\wp_5	19-12-2001	5221.96	\wp_{11}
20-11-2001	4455.80	\wp_4	20-12-2001	5309.10	\wp_{12}
21-11-2001	4533.37	\wp_5	21-12-2001	5109.24	\wp_{10}
22-11-2001	4450.02	\wp_4	24-12-2001	5164.73	\wp_{10}
23-11-2001	4519.08	\wp_5	25-12-2001	5372.81	\wp_{12}
26-11-2001	4608.32	\wp_6	26-12-2001	5392.43	\wp_{12}
27-11-2001	4580.33	\wp_6	27-12-2001	5332.98	\wp_{12}
28-11-2001	4447.58	\wp_4	28-12-2001	5398.28	\wp_{12}
29-11-2001	4465.83	\wp_5	31-12-2001	5551.24	\wp_{14}
30-11-2001	4441.12	\wp_4			

This segment delineates the application of the developed approach to Alzheimer's disease data from 2001, providing a systematic explanation of the results for easier interpretation and validation of the model. The methodology is outlined in the following steps:

Step I: Definition of the discourse universe

The discourse universe Ψ for the 2001 Alzheimer's patient data is defined as [3920, 5600]. This range is determined using the minimum (A_{\min}) and maximum (A_{\max}) values from Table 1, adjusted by two chosen positive numbers $A_1 = 9.69$ and $A_2 = 48.76$.

Step II: Segmentation of the discourse universe

The universe Ψ is divided into 14 intervals, denoted as $\tilde{h}_v = [3920 + (v - 1)p, 3920 + vp]$, $v = 1, 2, 3, \dots, 14$ and $p = 120$.

Step III: Establishment of C-PyFSTS

Fourteen C-PyFSTS, $\wp_v (v = 1, 2, 3, \dots, 14)$, are established within the discourse universe based on the interval \tilde{h}_v . The C-PyFSTS are determined as follows:

$$\wp_v = [3920+(v-1)p, 3920+vp, 3920+(i+1)p] \text{ for } v = 1, 2, 3, \dots, 13 \text{ where } p = 120$$

$$\wp_v = [3920+(v-1)p, 3920+vp, 3920+ip] \text{ for } v = 14 \text{ where } p = 120$$

Membership and non-membership values to C-PyFSTS are calculated using Eqs. (3) and (4), assuming $\epsilon = 0.001$.

$$\wp_1 = \{(3929.69, 0.08, 0.92), (3998.48, 0.65, 0.35), (4080.51, 0.66, 0.34), (4082.92, 0.64, 0.36), (4158.15, 0.01, 0.99), (4135.03, 0.21, 0.79), (4123.78, 0.30, 0.70), (4136.54, 0.19, 0.81)\}$$

$$\wp_2 = \{(4080.51, 0.34, 0.66), (4082.92, 0.36, 0.64), (4158.15, 0.97, 0.03), (4135.03, 0.79, 0.21), (4123.78, 0.70, 0.30), (4172.63, 0.89, 0.11), (4136.54, 0.80, 0.20), (4277.70, 0.02, 0.98)\}$$

$$\wp_3 = \{(4172.63, 0.10, 0.90), (4277.70, 0.98, 0.02)\}$$

$$\begin{aligned}
\wp_4 &= \{(4403.59, 0.97, 0.03), (4446.62, 0.61, 0.39), (4455.80, 0.53, 0.47), (4450.02, 0.58, 0.42), (4159.08, 0.01, 0.99), \\
&\quad (4447.58, 0.60, 0.40), (4465.83, 0.45, 0.55), (4441.12, 0.66, 0.34)\} \\
\wp_5 &= \{(4403.59, 0.03, 0.97), (4446.62, 0.39, 0.61), (4548.63, 0.76, 0.53), (4455.80, 0.46, 0.54), (4533.37, 0.89, \\
&\quad 0.11), (4450.02, 0.42, 0.58), (4519.08, 0.99, 0.01), (4608.32, 0.26, 0.74), (4580.33, 0.50, 0.50), (4447.58, 0.40, \\
&\quad 0.60), (4465.83, 0.55, 0.45), (4441.61, 0.35, 0.65)\} \\
\wp_6 &= \{(4548.63, 0.24, 0.76), (4533.37, 0.11, 0.89), (4608.32, 0.73, 0.27), (4580.33, 0.50, 0.50), (4646.61, 0.94, 0.06)\} \\
\wp_7 &= \{(4646.61, 0.05, 0.95), (4766.43, 0.95, 0.05)\} \\
\wp_8 &= \{(4766.43, 0.05, 0.95), (4924.56, 0.63, 0.37)\} \\
\wp_9 &= \{(4924.56, 0.37, 0.63), (5109.24, 0.09, 0.91)\} \\
\wp_{10} &= \{(5208.86, 0.26, 0.74), (5221.96, 0.15, 0.85), (5109.24, 0.91, 0.09), (5164.73, 0.63, 0.37)\} \\
\wp_{11} &= \{(5208.86, 0.74, 0.26), (5333.93, 0.22, 0.78), (5329.19, 0.26, 0.74), (5221.96, 0.85, 0.15), (5309.10, 0.42, \\
&\quad 0.58), (5164.73, 0.37, 0.63), (5332.98, 0.22, 0.78), (5273.97, 0.72, 0.28), (5321.28, 0.32, 0.68)\} \\
\wp_{12} &= \{(5333.93, 0.78, 0.22), (5407.54, 0.60, 0.40), (5456.15, 0.20, 0.80), (5329.19, 0.74, 0.26), (5309.10, 0.57, \\
&\quad 0.43), (5372.81, 0.89, 0.11), (5392.43, 0.73, 0.27), (5332.98, 0.77, 0.23), (5398.28, 0.68, 0.32), (5321.28, \\
&\quad 0.68, 0.32), (5273.97, 0.28, 0.72)\} \\
\wp_{13} &= \{(5407.54, 0.40, 0.60), (5486.73, 0.94, 0.06), (5456.15, 0.80, 0.20), (5372.81, 0.11, 0.89), (5392.43, 0.27, \\
&\quad 0.73), (5398.28, 0.32, 0.68), (5551.24, 0.41, 0.59), (5539.31, 0.50, 0.50)\} \\
\wp_{14} &= \{(5486.73, 0.06, 0.94), (5551.24, 0.59, 0.41), (5539.31, 0.49, 0.51)\}
\end{aligned}$$

Step IV: Calculation of the radius of C-PyFSs

The radius for each C-PyFS is calculated utilizing Eqs. (5) and (6).

$$\begin{aligned}
\wp_1 &= \{(3929.69 (0.08, 0.92; 0.37)), (3998.48 (0.65, 0.35; 0.44)), (4080.51 (0.66, 0.34; 0.45)), (4082.92 (0.64, 0.36; 0.42)), \\
&\quad (4158.15 (0.01, 0.99; 0.47)), (4135.03 (0.21, 0.79; 0.19)), (4123.78 (0.30, 0.70; 0.06)), (4136.54 (0.19, 0.81; \\
&\quad 0.21))\} \\
\wp_2 &= \{(4080.51 (0.34, 0.66; 0.39)), (4082.92 (0.36, 0.64; 0.36)), (4158.15 (0.97, 0.03; 0.52)), (4135.03 (0.79, 0.21; \\
&\quad 0.26)), (4123.78 (0.70, 0.30; 0.12)), (4172.63 (0.89, 0.11; 0.40)), (4136.54 (0.80, 0.20; 0.28)), (4277.70 (0.02, \\
&\quad 0.98; 0.84))\} \\
\wp_3 &= \{(4172.63 (0.10, 0.90; 0.62)), (4277.70 (0.98, 0.02, 0.62))\} \\
\wp_4 &= \{(4403.59 (0.97, 0.03; 0.59)), (4446.62 (0.61, 0.39; 0.08)), (4455.80 (0.53, 0.47; 0.02)), (4450.02 (0.58, 0.42; \\
&\quad 0.04)), (4159.08 (0.01, 0.99; 0.77)), (4447.58 (0.60, 0.40; 0.07)), (4465.83 (0.45, 0.55; 0.14)), (4441.12 \\
&\quad (0.66, 0.34; 0.15))\} \\
\wp_5 &= \{(4403.59 (0.03, 0.97; 0.65)), (4446.62 (0.39, 0.61; 0.14)), (4548.63 (0.76, 0.53; 0.26)), (4455.80 (0.46, 0.54; \\
&\quad 0.04)), (4533.37 (0.89, 0.11; 0.57)), (4450.02 (0.42, 0.58; 0.10)), (4519.08 (0.99, 0.01; 0.71)), (4608.32 \\
&\quad (0.26, 0.74; 0.32)), (4580.33 (0.50, 0.50; 0.02)), (4447.58 (0.40, 0.60 : 0.13)), (4465.83 (0.55, 0.45; 0.09)), \\
&\quad (4441.61 (0.35, 0.65; 0.20))\} \\
\wp_6 &= \{(4548.63 (0.24, 0.76; 0.38)), (4533.37 (0.11, 0.89; 0.56)), (4608.32 (0.73, 0.27; 0.32)), (4580.33 (0.50, 0.50; \\
&\quad 0.01)), (4646.61 (0.94, 0.06; 0.62))\} \\
\wp_7 &= \{(4646.61 (0.05, 0.95; 0.63)), (4766.43 (0.95, 0.05; 0.63))\} \\
\wp_8 &= \{(4766.43 (0.05, 0.95; 0.41)), (4924.56 (0.63, 0.37; 0.41))\} \\
\wp_9 &= \{(4924.56 (0.37, 0.63; 0.20)), (5109.24 (0.09, 0.91; 0.20))\} \\
\wp_{10} &= \{(5208.86 (0.26, 0.74; 0.32)), (5221.96 (0.15, 0.85; 0.48)), (5109.24 (0.91, 0.09; 0.60)), (5164.73 (0.63, 0.37; \\
&\quad 0.20))\} \\
\wp_{11} &= \{(5208.86 (0.74, 0.26; 0.40)), (5333.93 (0.22, 0.78; 0.34)), (5329.19 (0.26, 0.74; 0.29)), (5221.96 (0.85, 0.15; \\
&\quad 0.55)), (5309.10 (0.42, 0.58; 0.05)), (5164.73 (0.37, 0.63; 0.12)), (5332.98 (0.22, 0.78; 0.33)), (5273.97 (0.72, \\
&\quad 0.28; 0.37)), (5321.28 (0.32, 0.68; 0.19))\} \\
\wp_{12} &= \{(5333.93 (0.78, 0.22; 0.13)), (5407.54 (0.60, 0.40; 0.13)), (5456.15 (0.20, 0.80; 0.70)), (5329.19 (0.74, 0.26; \\
&\quad 0.07)), (5309.10 (0.57, 0.43; 0.17)), (5372.81 (0.89, 0.11; 0.28)), (5392.43 (0.73, 0.27; 0.05)), (5332.98 (0.77, \\
&\quad 0.23; 0.12)), (5398.28 (0.68, 0.32; 0.02)), (5321.28 (0.68, 0.32; 0.02)), (5273.97 (0.28, 0.72; 0.58))\} \\
\wp_{13} &= \{(5407.54 (0.40, 0.60; 0.10)), (5486.73 (0.94, 0.06; 0.67)), (5456.15 (0.80, 0.20; 0.47)), (5372.81 (0.11, 0.89; \\
&\quad 0.51)), (5392.43 (0.27, 0.73; 0.28)), (5398.28 (0.32, 0.68; 0.21)), (5551.24 (0.41, 0.59; 0.09)), (5539.31 (0.50, \\
&\quad 0.50; 0.05))\} \\
\wp_{14} &= \{(5486.73 (0.06, 0.94; 0.46)), (5551.24 (0.59, 0.41; 0.30)), (5539.31 (0.49, 0.51; 0.16))\}
\end{aligned}$$

Step V: Computation of the C-PyFS score value

The score value for each data point within the C-PyFS is calculated using Eq.(7). For instance, the score degree for the actual value of 4080.51, located between the circular Pythagorean membership and non-membership values of \wp_1 and \wp_2 , is ascertained.

In the process of determining the highest score degree for the specific data point of 4080.51, the methodological steps outlined in Step IV were employed. These steps involve the calculation of membership,

non-membership, and radii values for the C-PyFS. For the purpose of this calculation, it is assumed that the parameter p has a value of 0.5

$$\mu_{\wp_1}(4080.51) = 0.66, \nu_{\wp_1}(4080.51) = 0.34, r_{\wp_1}(4080.51) = 0.45$$

Similarly,

$$\mu_{\wp_2}(4080.51) = 0.34, \nu_{\wp_2}(4080.51) = 0.66, r_{\wp_2}(4080.51) = 0.39$$

The score degree for the data point 4080.51 was then calculated for both \wp_1 and \wp_2 . Then the larger value was selected.

$$\zeta_{\wp_1}(4080.51) = \frac{1}{3}(0.66 - 0.34 + \sqrt{2 \times 0.45}(2 \times 0.5 - 1)) = 0.11$$

$$\zeta_{\wp_2}(4080.51) = \frac{1}{3}(0.34 - 0.66 + \sqrt{2 \times 0.39}(2 \times 0.5 - 1)) = -0.11$$

Given that \wp_1 exhibited a higher score degree than \wp_2 , \wp_1 was determined to be the circular Pythagorean value for the data point 4080.51. Subsequent calculations followed a similar procedure for the remaining data points.

Step VI: Formulation of circular Pythagorean logical relationships (C-PLRs)

C-PLRs are established and presented in Table 2.

Table 2. C-PLRs of order I

$\wp_1 \rightarrow \wp_1$	$\wp_1 \rightarrow \wp_1$	$\wp_1 \rightarrow \wp_1$	$\wp_1 \rightarrow \wp_2$	$\wp_2 \rightarrow \wp_2$	$\wp_2 \rightarrow \wp_2$	$\wp_2 \rightarrow \wp_2$
$\wp_2 \rightarrow \wp_2$	$\wp_2 \rightarrow \wp_3$	$\wp_3 \rightarrow \wp_4$	$\wp_4 \rightarrow \wp_4$	$\wp_4 \rightarrow \wp_5$	$\wp_5 \rightarrow \wp_4$	$\wp_4 \rightarrow \wp_5$
$\wp_5 \rightarrow \wp_4$	$\wp_4 \rightarrow \wp_5$	$\wp_5 \rightarrow \wp_6$	$\wp_6 \rightarrow \wp_6$	$\wp_6 \rightarrow \wp_4$	$\wp_4 \rightarrow \wp_5$	$\wp_5 \rightarrow \wp_4$
$\wp_4 \rightarrow \wp_6$	$\wp_6 \rightarrow \wp_7$	$\wp_7 \rightarrow \wp_8$	$\wp_8 \rightarrow \wp_{11}$	$\wp_{11} \rightarrow \wp_{12}$	$\wp_{12} \rightarrow \wp_{12}$	$\wp_{12} \rightarrow \wp_{11}$
$\wp_{11} \rightarrow \wp_{13}$	$\wp_{13} \rightarrow \wp_{12}$	$\wp_{12} \rightarrow \wp_{13}$	$\wp_{13} \rightarrow \wp_{13}$	$\wp_{13} \rightarrow \wp_{12}$	$\wp_{12} \rightarrow \wp_{11}$	$\wp_{11} \rightarrow \wp_{12}$
$\wp_{12} \rightarrow \wp_{10}$	$\wp_{10} \rightarrow \wp_{10}$	$\wp_{10} \rightarrow \wp_{12}$	$\wp_{12} \rightarrow \wp_{12}$	$\wp_{12} \rightarrow \wp_{12}$	$\wp_{12} \rightarrow \wp_{12}$	$\wp_{12} \rightarrow \wp_{14}$

Step VII: Creation of C-PyFLRGs

Building upon the C-PLRs, C-PyFLRGs are developed. These groups are displayed in Table 3.

Table 3. C-PyFLRGs of order I

$\wp_1 \rightarrow \wp_1$	$\wp_1 \rightarrow \wp_1$	$\wp_1 \rightarrow \wp_1$	$\wp_1 \rightarrow \wp_2$						
$\wp_2 \rightarrow \wp_2$	$\wp_2 \rightarrow \wp_2$	$\wp_2 \rightarrow \wp_2$	$\wp_2 \rightarrow \wp_2$	$\wp_2 \rightarrow \wp_3$					
$\wp_3 \rightarrow \wp_4$									
$\wp_4 \rightarrow \wp_4$	$\wp_4 \rightarrow \wp_5$	$\wp_4 \rightarrow \wp_5$	$\wp_4 \rightarrow \wp_5$	$\wp_4 \rightarrow \wp_5$	$\wp_4 \rightarrow \wp_6$				
$\wp_5 \rightarrow \wp_4$	$\wp_5 \rightarrow \wp_4$	$\wp_5 \rightarrow \wp_6$	$\wp_5 \rightarrow \wp_4$						
$\wp_6 \rightarrow \wp_6$	$\wp_6 \rightarrow \wp_4$	$\wp_6 \rightarrow \wp_7$							
$\wp_7 \rightarrow \wp_8$									
$\wp_8 \rightarrow \wp_{11}$									
$\wp_{10} \rightarrow \wp_{10}$	$\wp_{10} \rightarrow \wp_{12}$								
$\wp_{11} \rightarrow \wp_{12}$	$\wp_{11} \rightarrow \wp_{13}$	$\wp_{11} \rightarrow \wp_{12}$							
$\wp_{12} \rightarrow \wp_{12}$	$\wp_{12} \rightarrow \wp_{11}$	$\wp_{12} \rightarrow \wp_{13}$	$\wp_{12} \rightarrow \wp_{11}$	$\wp_{12} \rightarrow \wp_{12}$	$\wp_{12} \rightarrow \wp_{14}$				
$\wp_{13} \rightarrow \wp_{12}$	$\wp_{13} \rightarrow \wp_{13}$	$\wp_{13} \rightarrow \wp_{12}$							

4.1 Computation of Forecasted Values Using C-PyFSs

Table 4 presents the forecasted values derived from the C-PyFSs model. Due to the absence of an initial value on November 1, 2001, the model was unable to generate a forecast for that date. Subsequently, forecasted values for the following days were computed using the established methodology.

Table 4. Forecasted value of Alzheimer’s disease of order I

Date	True Value	Forecasted Value	Year	True Value	Forecasted Value
01-11-2001	3929.69	—	03-12-2001	4646.61	4520
02-11-2001	3998.48	4100	04-12-2001	4766.43	4600
05-11-2001	4080.51	4100	05-12-2001	4924.56	4880
06-11-2001	4082.92	4100	06-12-2001	5208.86	5240
07-11-2001	4158.15	4100	07-12-2001	5333.93	5360
08-11-2001	4135.03	4220	10-12-2001	5321.28	5420
09-11-2001	4123.78	4220	11-12-2001	5273.97	5420
12-11-2001	4172.63	4220	12-12-2001	5539.31	5420
13-11-2001	4136.54	4220	13-12-2001	5407.54	5420
14-11-2001	4277.70	4220	14-12-2001	5486.73	5420
15-11-2001	4403.59	4400	17-12-2001	5456.15	5420
16-11-2001	4446.62	4520	18-12-2001	5329.19	5420
19-11-2001	4548.63	4520	19-12-2001	5221.96	5420
20-11-2001	4455.80	4520	20-12-2001	5309.10	5420
21-11-2001	4533.37	4520	21-12-2001	5109.24	5420
22-11-2001	4450.02	4520	24-12-2001	5164.73	5240
23-11-2001	4519.08	4520	25-12-2001	5372.81	5240
26-11-2001	4608.32	4520	26-12-2001	5392.43	5420
27-11-2001	4580.33	4600	27-12-2001	5332.98	5420
28-11-2001	4447.58	4600	28-12-2001	5398.28	5420
29-11-2001	4465.83	4520	31-12-2001	5551.24	5420
30-11-2001	4441.12	4520			

Figure 1 depicts a graphical representation of both the actual and forecasted values related to Alzheimer’s disease cases.

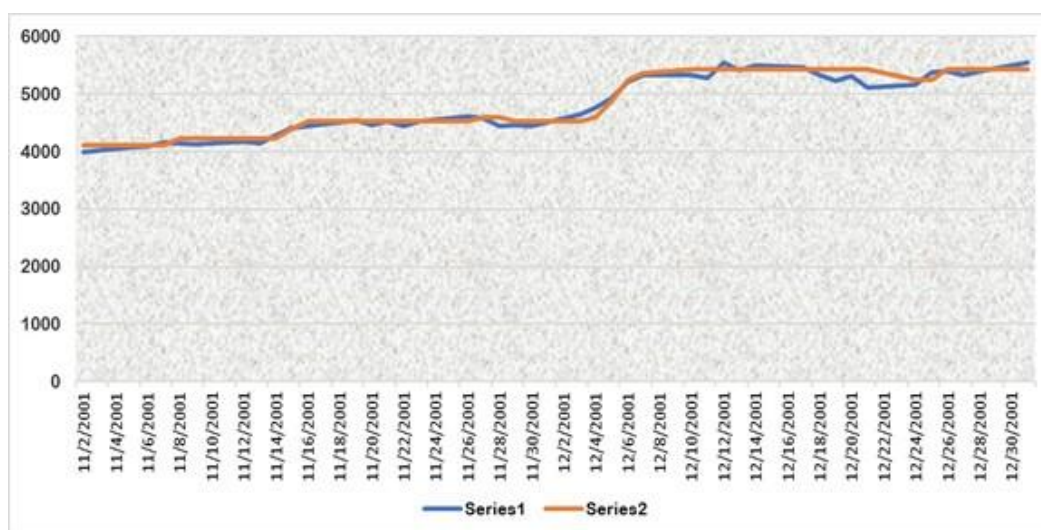


Figure 1. True and observed values of order I

5. Circular Pythagorean Logical Relationships (C-PLRs) of Order II

In this section, the methodology extends to constructing the C-PLRs and their corresponding groups for second-order forecasting in Alzheimer’s disease. The Table 5 delineates the C-PLRs for order II Alzheimer’s disease forecasting.

Table 5. C-PLRs of order II

$\wp_1, \wp_1 \rightarrow \wp_1$	$\wp_1, \wp_1 \rightarrow \wp_1$	$\wp_1, \wp_1 \rightarrow \wp_2$	$\wp_1, \wp_2 \rightarrow \wp_2$	$\wp_2, \wp_2 \rightarrow \wp_2$	$\wp_2, \wp_2 \rightarrow \wp_2$
$\wp_2, \wp_2 \rightarrow \wp_2$	$\wp_2, \wp_2 \rightarrow \wp_3$	$\wp_2, \wp_3 \rightarrow \wp_4$	$\wp_3, \wp_4 \rightarrow \wp_4$	$\wp_4, \wp_4 \rightarrow \wp_5$	$\wp_4, \wp_5 \rightarrow \wp_4$
$\wp_5, \wp_4 \rightarrow \wp_5$	$\wp_4, \wp_5 \rightarrow \wp_4$	$\wp_5, \wp_4 \rightarrow \wp_5$	$\wp_4, \wp_5 \rightarrow \wp_6$	$\wp_5, \wp_6 \rightarrow \wp_6$	$\wp_6, \wp_6 \rightarrow \wp_4$
$\wp_6, \wp_4 \rightarrow \wp_5$	$\wp_4, \wp_5 \rightarrow \wp_4$	$\wp_5, \wp_4 \rightarrow \wp_6$	$\wp_4, \wp_6 \rightarrow \wp_7$	$\wp_6, \wp_7 \rightarrow \wp_8$	$\wp_7, \wp_8 \rightarrow \wp_{11}$
$\wp_8, \wp_{11} \rightarrow \wp_{12}$	$\wp_{11}, \wp_{12} \rightarrow \wp_{12}$	$\wp_{12}, \wp_{12} \rightarrow \wp_{11}$	$\wp_{12}, \wp_{11} \rightarrow \wp_{13}$	$\wp_{11}, \wp_{13} \rightarrow \wp_{12}$	$\wp_{13}, \wp_{12} \rightarrow \wp_{13}$
$\wp_{12}, \wp_{13} \rightarrow \wp_{13}$	$\wp_{13}, \wp_{13} \rightarrow \wp_{12}$	$\wp_{13}, \wp_{12} \rightarrow \wp_{11}$	$\wp_{12}, \wp_{11} \rightarrow \wp_{12}$	$\wp_{11}, \wp_{12} \rightarrow \wp_{10}$	$\wp_{12}, \wp_{10} \rightarrow \wp_{10}$
$\wp_{10}, \wp_{10} \rightarrow \wp_{12}$	$\wp_{10}, \wp_{12} \rightarrow \wp_{12}$	$\wp_{12}, \wp_{12} \rightarrow \wp_{12}$	$\wp_{12}, \wp_{12} \rightarrow \wp_{12}$	$\wp_{12}, \wp_{12} \rightarrow \wp_{14}$	

Based on the C-PLRs, Table 6 presents the C-PyFLRGs for order II.

Table 6. Circular Pythagorean logical relationship groups of order II

$\wp_1, \wp_1 \rightarrow \wp_1$	$\wp_1, \wp_1 \rightarrow \wp_1$	$\wp_1, \wp_1 \rightarrow \wp_2$		$\wp_1, \wp_2 \rightarrow \wp_2$	
$\wp_2, \wp_2 \rightarrow \wp_2$	$\wp_2, \wp_2 \rightarrow \wp_2$	$\wp_2, \wp_2 \rightarrow \wp_2$	$\wp_2, \wp_2 \rightarrow \wp_3$	$\wp_2, \wp_3 \rightarrow \wp_4$	
$\wp_3, \wp_4 \rightarrow \wp_4$				$\wp_4, \wp_4 \rightarrow \wp_5$	
$\wp_4, \wp_5 \rightarrow \wp_4$	$\wp_4, \wp_5 \rightarrow \wp_4$	$\wp_4, \wp_5 \rightarrow \wp_6$	$\wp_4, \wp_5 \rightarrow \wp_4$	$\wp_5, \wp_4 \rightarrow \wp_5$	$\wp_5, \wp_4 \rightarrow \wp_5$
$\wp_5, \wp_6 \rightarrow \wp_6$				$\wp_6, \wp_6 \rightarrow \wp_4$	$\wp_5, \wp_4 \rightarrow \wp_6$
$\wp_6, \wp_4 \rightarrow \wp_5$				$\wp_4, \wp_6 \rightarrow \wp_7$	
$\wp_6, \wp_7 \rightarrow \wp_8$				$\wp_7, \wp_8 \rightarrow \wp_{11}$	
$\wp_8, \wp_{11} \rightarrow \wp_{12}$				$\wp_{11}, \wp_{11} \rightarrow \wp_{12}$	$\wp_{11}, \wp_{12} \rightarrow \wp_{10}$
$\wp_{12}, \wp_{12} \rightarrow \wp_{11}$	$\wp_{12}, \wp_{12} \rightarrow \wp_{12}$	$\wp_{12}, \wp_{12} \rightarrow \wp_{12}$	$\wp_{12}, \wp_{12} \rightarrow \wp_{14}$	$\wp_{12}, \wp_{11} \rightarrow \wp_{13}$	$\wp_{12}, \wp_{11} \rightarrow \wp_{12}$
$\wp_{11}, \wp_{13} \rightarrow \wp_{12}$				$\wp_{13}, \wp_{12} \rightarrow \wp_{13}$	$\wp_{13}, \wp_{12} \rightarrow \wp_{11}$
$\wp_{12}, \wp_{13} \rightarrow \wp_{13}$				$\wp_{13}, \wp_{13} \rightarrow \wp_{12}$	
$\wp_{12}, \wp_{10} \rightarrow \wp_{10}$				$\wp_{10}, \wp_{10} \rightarrow \wp_{12}$	
$\wp_{10}, \wp_{10} \rightarrow \wp_{12}$					

5.1 Determination of Forecasted Value of C-PyFSS

Table 7 illustrates the forecasted values for Alzheimer's disease, computed using the second-order C-PyFSS as outlined in Section B.

Table 7. Forecasted value of Alzheimer's disease of order II

Date	True Value	Forecasted Value	Years	True Value	Forecasted Value
01-11-2001	3929.69	—	03-12-2001	4646.61	4580
02-11-2001	3998.48	—	04-12-2001	4766.43	4760
05-11-2001	4080.51	4100	05-12-2001	4924.56	4880
06-11-2001	4082.92	4100	06-12-2001	5208.86	5240
07-11-2001	4158.15	4100	07-12-2001	5333.93	5360
08-11-2001	4135.03	4160	10-12-2001	5321.2	5240
09-11-2001	4123.78	4220	11-12-2001	5273.97	5400
12-11-2001	4172.63	4220	12-12-2001	5539.31	5420
13-11-2001	4136.54	4220	13-12-2001	5407.54	5360
14-11-2001	4277.70	4220	14-12-2001	5486.73	5360
15-11-2001	4403.59	4400	17-12-2001	5456.15	5480
16-11-2001	4446.62	4400	18-12-2001	5329.19	5360
19-11-2001	4548.63	4520	19-12-2001	5221.96	5360
20-11-2001	4455.80	4520	20-12-2001	5309.10	5420
21-11-2001	4533.37	4580	21-12-2001	5109.24	5420
22-11-2001	4450.02	4520	24-12-2001	5164.73	5120
23-11-2001	4519.08	4580	25-12-2001	5372.81	5360
26-11-2001	4608.32	4520	26-12-2001	5392.43	5360
27-11-2001	4580.33	4640	27-12-2001	5332.98	5400
28-11-2001	4447.58	4400	28-12-2001	5398.28	5400
29-11-2001	4465.83	4520	31-12-2001	5551.24	5400
30-11-2001	4441.12	4520			

A graphical representation, Figure 2, compares the actual values with the forecasted values for Alzheimer's disease using the second-order C-PyFS approach.

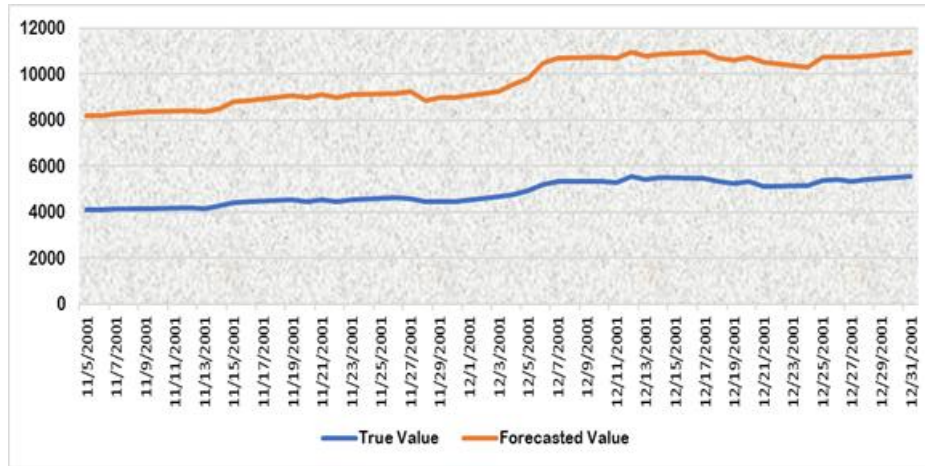


Figure 2. Graph of the actual and forecasted values of order II

5.2 Measurement of Error Using RMSE and AFE

To assess the accuracy of the forecasts, Table 8 presents the calculations for RMSE and AFE. These metrics are crucial for evaluating the precision of the forecasting method.

Table 8. RMSE and AFE for first and second-order forecasting methods

Tools	Proposed Method (Order I)	Proposed Method (Order II)
MSE	98.03	84.61
AFE	1.61	1.34

6. Discussion

The results delineated in Table 8 articulate a comparative analysis between first- and second-order C-PyFTS forecasting. It has been observed that the second-order C-PyFTS forecasting demonstrates a superior performance over the first-order model, as evidenced by the calculated error rates using established error measurement formulas.

A notable trend is observed in the forecasting accuracy: higher-order C-PyFTS models tend to yield lower error rates. This pattern holds for the third-order forecasting error, which is smaller than that of the second-order. This indicates that, generally, as the order increases, the accuracy of the C-PyFTS model improves, suggesting a more refined prediction capability. However, it is crucial to underscore that the quality and completeness of the data play a pivotal role in enhancing forecast accuracy, alongside the chosen forecasting methodology.

The RMSE value distinctly validates the efficacy of the proposed algorithm for addressing complex forecasting scenarios. The accuracy of the forecasting method, as manifested in the error metrics, has significant practical implications. Specifically, in the context of patient care within the neurological department, the application of the predictive analytics model enabled proactive patient management and optimized day-to-day operational efficiency. Anticipating patient inflow facilitated more effective resource allocation, ensuring optimal patient care.

The significance of the radius in C-PyFS extends beyond its traditional role in membership and non-membership determination. In C-PyFS, the radius is instrumental in influencing the overall dimensions and configuration of the fuzzy set. This, in turn, impacts the set's ability to represent intricate and uncertain data comprehensively, enhancing the model's adaptability and interpretability in handling complex fuzzy logic problems.

7. Conclusions

The study presented herein demonstrates the increasing preference for C-PyFSs when dealing with scenarios where the sum of membership and non-membership degrees is one or less. It has been discerned that traditional PyFSs are inadequate in addressing such cases, leading to the utilization of C-PyFSs in instances where the aggregate of membership and non-membership values equals one. The proposed approach utilizing C-PyFSs has been identified as less complex and more straightforward, primarily due to the adoption of a simplified scoring formula. This methodology was applied to forecast the indices of Alzheimer's disease, demonstrating its utility

in predicting data using the established criteria. Furthermore, the extension of this approach to higher-order forecasts revealed that higher-order predictions are characterized by reduced errors, thereby enhancing their utility in future value estimations.

The application of the recommended strategy yielded predictions for the ensuing years, indicating its potential for extensive use in various forecasting scenarios. Future research avenues may explore the application of C-PyFSs across diverse time-series forecasting problems, comparing their efficacy against existing methodologies. Such investigations could offer additional insights and enhancements to the forecasting process, broadening the scope and applicability of C-PyFSs in diverse research and practical domains.

Ethical Approval

This article does not contain any studies with human participants or animals performed by any of the authors.

Data Availability

The data used to support the research findings are available from the corresponding author upon request.

Conflicts of Interest

The authors declare no conflict of interest.

References

- Abhishekh, Gautam, S. S. & Singh, S. R. (2018). A refined method of forecasting based on high-order intuitionistic fuzzy time series data. *Prog. Artif. Intell.*, 7, 339-350. <https://doi.org/10.1007/s13748-018-0152-x>.
- Ashraf, S., Abdullah, S., & Almagrabi, A. O. (2020). A new emergency response of spherical intelligent fuzzy decision process to diagnose of COVID-19. *Soft Comput.*, 27(3), 1809–1825. <https://doi.org/10.1007/s00500-020-05287-8>.
- Ashraf, S., Abdullah, S., Aslam, M., Qiyas, M., & Kutbi, M. A. (2019a). Spherical fuzzy sets and its representation of spherical fuzzy t-norms and t-conorms. *J. Intell. Fuzzy Syst.*, 36(6), 6089-6102. <https://doi.org/10.3233/JIFS-181941>.
- Ashraf, S., Abdullah, S., Mahmood, T., Ghani, F., & Mahmood, T. (2019b). Spherical fuzzy sets and their applications in multi-attribute decision making problems. *J. Intell. Fuzzy Syst.*, 36(3), 2829-2844. <https://doi.org/10.3233/JIFS-172009>.
- Ashraf, S., Chohan, M. S., Ahmad, S., Hameed, M. S., & Khan, F. (2023a). Decision aid algorithm for kidney transplants under disc spherical fuzzy sets with distinctive radii information. *IEEE Access*, 11, 122029-122044. <https://doi.org/10.1109/ACCESS.2023.3327830>.
- Ashraf, S., Chohan, M. S., Muhammad, S., & Khan, F. (2023b). Circular intuitionistic fuzzy TODIM approach for material selection for cryogenic storage tank for liquid nitrogen transportation. *IEEE Access*, 11, 98458-98468. <https://doi.org/10.1109/ACCESS.2023.3312568>.
- Atanassov, K. T. (1999). *Intuitionistic Fuzzy Sets*. Physica, Heidelberg. https://doi.org/10.1007/978-3-7908-1870-3_1.
- Atanassov, K. T. (2007). Remark on intuitionistic fuzzy numbers. *Notes on Intuitionistic Fuzzy Sets*, 13(3), 29-32.
- Athar, H. M. A. & Riaz, M. (2022). Innovative q -rung orthopair fuzzy prioritized interactive aggregation operators to evaluate efficient autonomous vehicles for freight transportation. *Scientia Iranica*. <https://doi.org/10.24200/sci.2022.59601.6326>.
- Attaullah, Ashraf, S., Rehman, N., AlSalman, H., & Gumaei, A. H. (2022). A decision-making framework using q -rung orthopair probabilistic hesitant fuzzy rough aggregation information for the drug selection to treat COVID-19. *Complexity*, 2022, 1-37. <https://doi.org/10.1155/2022/5556309>.
- Çakır, E., Tas, M. A., & Ulukan, Z. (2022). Circular intuitionistic fuzzy sets in multi criteria decision making. In 11th International Conference on Theory and Application of Soft Computing, Computing with Words and Perceptions and Artificial Intelligence-ICSCCW-2021, Antalya, Turkey, pp. 34–42. https://doi.org/10.1007/978-3-030-92127-9_9.
- Chen, S. M. (1996). Forecasting enrollments based on fuzzy time series. *Fuzzy Sets Syst.*, 81(3), 311-319. [https://doi.org/10.1016/0165-0114\(95\)00220-0](https://doi.org/10.1016/0165-0114(95)00220-0).
- Chen, T. Y. (2023). A circular intuitionistic fuzzy evaluation method based on distances from the average solution to support multiple criteria intelligent decisions involving uncertainty. *Eng. Appl. Artif. Intell.*, 117, 105499. <https://doi.org/10.1016/j.engappai.2022.105499>.

- Cheng, C. H., Cheng, G. W., & Wang, J. W. (2008). Multi-attribute fuzzy time series method based on fuzzy clustering. *Expert Syst. Appl.*, *34*(2), 1235-1242. <https://doi.org/10.1016/j.eswa.2006.12.013>.
- Chinram, R., Ashraf, S., Abdullah, S., & Petchkaew, P. (2020). Decision support technique based on spherical fuzzy Yager aggregation operators and their application in wind power plant locations: A case study of Jhimpir, Pakistan. *J. Math.*, 2020, 1-21. <https://doi.org/10.1155/2020/8824032>.
- Chou, M. T. (2011). Long-term predictive value interval with the fuzzy time series. *J. Mar. Sci. Technol.*, *19*(5), 6. <https://doi.org/10.51400/2709-6998.2164>.
- Cuong, B. C. & Kreinovich, V. (2013). Picture fuzzy sets - A new concept for computational intelligence problems. In 2013 Third World Congress on Information and Communication Technologies (WICT 2013), Hanoi, Vietnam, pp. 1-6. <https://doi.org/10.1109/WICT.2013.7113099>.
- Dutta, P. (2017). Medical diagnosis via distance measures on picture fuzzy sets. *Adv. Model. Anal. A*, *54*(2), 657-672.
- Farid, H. M. A. & Riaz, M. (2023). q-rung orthopair fuzzy Aczel-Alsina aggregation operators with multi-criteria decision-making. *Eng. Appl. Artif. Intell.*, *122*, 106105. <https://doi.org/10.1016/j.engappai.2023.106105>.
- Farid, H. M. A., Riaz, M., Almohsin, B., & Marinkovic, D. (2023). Optimizing filtration technology for contamination control in gas processing plants using hesitant q-rung orthopair fuzzy information aggregation. *Soft Comput.*, 1-26. <https://doi.org/10.1007/s00500-023-08588-w>.
- Gangwar, S. S. & Kumar, S. (2014). Probabilistic and intuitionistic fuzzy sets-based method for fuzzy time series forecasting. *Cybern. Syst.*, *45*(4), 349-361. <https://doi.org/10.1080/01969722.2014.904135>.
- Garg, H. (2017). Some picture fuzzy aggregation operators and their applications to multicriteria decision-making. *Arab. J. Sci. Eng.*, *42*(12), 5275-5290. <https://doi.org/10.1007/s13369-017-2625-9>.
- Gündoğdu, F. K. & Ashraf, S. (2021). Some novel preference relations for picture fuzzy sets and selection of 3-D printers in aviation 4.0. In *Intelligent and Fuzzy Techniques in Aviation 4.0: Theory and Applications*, pp. 281-300. https://doi.org/10.1007/978-3-030-75067-1_12.
- Jiang, P., Yang, H., & Heng, J. (2019). A hybrid forecasting system based on fuzzy time series and multi-objective optimization for wind speed forecasting. *Appl. Energy*, *235*, 786-801. <https://doi.org/10.1016/j.apenergy.2018.11.012>.
- Joshi, B. P. & Kumar, S. (2012a). A computational method of forecasting based on intuitionistic fuzzy sets and fuzzy time series. In *Proceedings of the International Conference on Soft Computing for Problem Solving (SocProS 2011)* (pp. 993-1000). https://doi.org/10.1007/978-81-322-0491-6_91.
- Joshi, B. P. & Kumar, S. (2012b). Intuitionistic fuzzy sets-based method for fuzzy time series forecasting. *Cybern. Syst.*, *43*(1), 34-47. <https://doi.org/10.1080/01969722.2012.637014>.
- Khan, M. J., Alcantud, J. C. R., Kumam, W., Kumam, P., & Alreshidi, N. A. (2023). Expanding Pythagorean fuzzy sets with distinctive radii: disc Pythagorean fuzzy sets. *Complex Intell. Syst.*, *9*(6), 7037-7054. <https://doi.org/10.1007/s40747-023-01062-y>.
- Khan, M. J., Kumam, W., & Alreshidi, N. A. (2022). Divergence measures for circular intuitionistic fuzzy sets and their applications. *Eng. Appl. Artif. Intell.*, *116*, 105455. <https://doi.org/10.1016/j.engappai.2022.105455>.
- Khan, S., Abdullah, S., Ashraf, S., Chinram, R., & Baupradist, S. (2020). Decision support technique based on neutrosophic Yager aggregation operators: Application in solar power plant locations—Case study of Bahawalpur, Pakistan. *Math. Probl. Eng.*, 2020, 1-21. <https://doi.org/10.1155/2020/6677676>.
- Kumar, S. & Gangwar, S. S. (2015a). A fuzzy time series forecasting method induced by intuitionistic fuzzy sets. *Int. J. Model. Simul. Sci. Comput.*, *6*(4), 1550041. <https://doi.org/10.1142/S1793962315500415>.
- Kumar, S. & Gangwar, S. S. (2015b). Intuitionistic fuzzy time series: An approach for handling nondeterminism in time series forecasting. *IEEE Trans. Fuzzy Syst.*, *24*(6), 1270-1281. <https://doi.org/10.1109/TFUZZ.2015.2507582>.
- Mahmood, T., Ullah, K., Khan, Q., & Jan, N. (2019). An approach toward decision-making and medical diagnosis problems using the concept of spherical fuzzy sets. *Neural Comput. Appl.*, *31*(11), 7041-7053. <https://doi.org/10.1007/s00521-018-3521-2>.
- Nayagam, V. L. G., Muralikrishnan, S., & Sivaraman, G. (2011). Multi-criteria decision-making method based on interval-valued intuitionistic fuzzy sets. *Expert Syst. Appl.*, *38*(3), 1464-1467. <https://doi.org/10.1016/j.eswa.2010.07.055>.
- Perçin, S. (2022). Circular supplier selection using interval-valued intuitionistic fuzzy sets. *Environ. Dev. Sustain.*, *24*(4), 5551-5581. <https://doi.org/10.1007/s10668-021-01671-y>.
- Riaz, M. & Farid, H. M. A. (2022). Hierarchical medical diagnosis approach for COVID-19 based on picture fuzzy fairly aggregation operators. *Int. J. Biomath.*, *16*(02), 2250075. <https://doi.org/10.1142/S1793524522500759>.
- Riaz, M., Farid, H. M. A., Alblowi, S. A., & Almalki, Y. (2022a). Novel concepts of q-rung orthopair fuzzy topology and WPM approach for multicriteria decision-making. *J. Funct. Spaces*, 2022.

- <https://doi.org/10.1155/2022/2094593>.
- Riaz, M., Farid, H. M. A., Wang, W., & Pamucar, D. (2022b). Interval-valued linear diophantine fuzzy Frank aggregation operators with multi-criteria decision-making. *Mathematics*, *10*(11), 1811. <https://doi.org/10.3390/math10111811>.
- Song, Q. & Chissom, B. S. (1993a). Forecasting enrollments with fuzzy time series - Part I. *Fuzzy Sets Syst.*, *54*(1), 1-9. [https://doi.org/10.1016/0165-0114\(93\)90355-L](https://doi.org/10.1016/0165-0114(93)90355-L).
- Song, Q. & Chissom, B. S. (1993b). Fuzzy time series and its models. *Fuzzy Sets Syst.*, *54*(3), 269-277. [https://doi.org/10.1016/0165-0114\(93\)90372-O](https://doi.org/10.1016/0165-0114(93)90372-O).
- Song, Q., & Chissom, B. S. (1994). Forecasting enrollments with fuzzy time series - Part II. *Fuzzy Sets Syst.*, *62*(1), 1-8. [https://doi.org/10.1016/0165-0114\(94\)90067-1](https://doi.org/10.1016/0165-0114(94)90067-1).
- Tan, C. (2011). A multi-criteria interval-valued Pythagorean fuzzy group decision making with Choquet integral-based TOPSIS. *Expert Syst. Appl.*, *38*(4), 3023-3033. <https://doi.org/10.1016/j.eswa.2010.08.092>.
- Ullah, K., Mahmood, T., & Jan, N. (2018). Similarity measures for T-spherical fuzzy sets with applications in pattern recognition. *Symmetry*, *10*(6), 193. <https://doi.org/10.3390/sym10060193>.
- Xu, Z. (2011). Approaches to multiple attribute group decision making based on intuitionistic fuzzy power aggregation operators. *Knowl. Based Syst.*, *24*(6), 749-760. <https://doi.org/10.1016/j.knosys.2011.01.011>.
- Yager, R. R. (2013). Pythagorean fuzzy subsets. In 2013 Joint IFSA World Congress and NAFIPS Annual Meeting (IFSA/NAFIPS), Edmonton, AB, Canada, pp. 57-61. <https://doi.org/10.1109/IFSA-NAFIPS.2013.6608375>.
- Zadeh, L. A., Klir, G. J., & Yuan, B. (1996). *Fuzzy Sets, Fuzzy Logic, and Fuzzy Systems: Selected Papers*. Singapore: World Scientific.